Band-gap tailoring of ZnO by means of heavy Al doping

B. E. Sernelius*
Solid State Division, Oak Ridge National Laboratory, Oak Ridge, Tennessee 37831
and Department of Physics, University of Tennessee, Knoxville, Tennessee 37996

K.-F. Berggren
Theoretical Physics Group, Department of Physics and Measurement Technology, Linköping University, S-581 83 Linköping, Sweden

Z.-C. Jin,† I. Hamberg,‡ and C. G. Granqvist
Physics Department, Chalmers University of Technology, S-412 96 Gothenburg, Sweden
(Received 30 November 1987)

Films of ZnO:Al were produced by weakly reactive dual-target magnetron sputtering. Optical band gaps, evaluated from spectrophotometric data, were widened in proportion to the Al doping. The widening could be quantitatively reconciled with an effective-mass model for *n*-doped semiconductors, provided the polar character of ZnO was accounted for.

I. INTRODUCTION AND SUMMARY

We analyze the optical properties of heavily Al-doped ZnO films, produced by sputtering, in the 2–5-eV range. The observed band-gap widening can be understood quantitatively from an effective-mass model for *n*-doped semiconductors. The present work is a sequel to our earlier study[1] of Sn-doped In_2O_3.

We are interested in a crystalline material which is doped to a sufficient level that the Mott critical density is exceeded.[2] The dopant atoms are then ionized and, for the case of *n* doping, the associated electrons occupy the bottom of the conduction band in the form of an electron gas. In principle, the optical band gap can be larger or smaller than the one of the undoped host crystal. A *widening* occurs since the lowest states in the conduction band are blocked; this is the well-known Burstein-Moss effect.[3] Band-gap *narrowing* is associated with different many-body effects on the conduction and valence bands.[4–6] Further, there may be effects of strain and other types of imperfection; they are not considered further here.

In an earlier study of ours[1] we analyzed band-gap widening in heavily Sn-doped In_2O_3 and argued that theory and experiments could be reconciled provided that the unknown effective valence-band mass of In_2O_3 was assigned a suitable value. Screening by the free electrons was described through the random-phase approximation or an extension thereof.[7] The screening due to the ions was represented by a static dielectric constant. The main purpose of the present work is to carry the analysis of band-gap shifts in heavily doped semiconductors further. We do this by studying thin films of doped zinc oxide. Crystalline ZnO has been carefully investigated in earlier work,[8] and its electron-band parameters are accurately known[9] at the pertinent ranges of energy and wave vector. Further, the present analysis includes the dynamics of ion-ion interaction and hence is more elaborate than in our earlier[1] study. As a secondary motivation for our present work, we may mention that band-gap tailoring at the ultraviolet end of the solar spectrum is of considerable interest for large-area optical coatings. These applications-oriented aspects, as well as the use of ZnO:Al as a low-emittance coating, are discussed elsewhere.[10]

In Sec. II below we report on the production of ZnO films containing up to 2 at. % Al using weakly reactive magnetron sputtering from two targets onto a rotating substrate. The spectral absorption coefficient was evaluated from spectrophotometric data for films with up to $\sim 5\times 10^{20}$ electrons per cm^3. Doping yielded a band-gap widening to as large as ~ 0.5 eV. Section III contains an outline of the theory for band-gap shifts in heavily doped semiconductors with emphasis on those aspects that are new for the current work. The theoretical model relies on the effective-mass approximation, i.e., wave functions are represented by plane waves, and the conduction and valence bands are taken to be parabolic near the center of the Brillouin zone. The ionized donors are described as point impurities, and the polar character for ZnO is accounted for explicitly. Theory and experiments are compared in Sec. IV. It is found that the band gaps obtained from the spectral absorption coefficients are in excellent accord with the theory, which, we want to stress, does not contain any free parameter. If not otherwise stated, cgs units are used.

II. EXPERIMENT

We made ZnO:Al films by simultaneous rf magnetron sputtering of ZnO (99.9% purity) and dc magnetron sputtering of Al (99.5% purity) in a versatile thin-film deposition unit.[11] Target diameters were 10 cm. Sputtering was conducted under weakly reactive conditions; specifically in 0.7 Pa of Ar (99.997% purity) mixed with O_2 (99.998% purity) to a ratio larger than 400:1. The

TABLE I. Data for doped ZnO films. Values are given on Al content, electron density (n_e) and optical band gap (E_g).

Sample	Material	Al content (at. %)	n_e (10^{20} cm^{-3})	E_g (eV)
A	ZnO	0	0.95	3.40
B	ZnO:Al	0.95	1.8	3.55
C	ZnO:Al	1.40	2.6	3.79
D	ZnO:Al	2.14	4.5	3.90

typical rf power was 150 W, whereas the dc power lay in the 0-7 W range. Substrates of CaF_2 (diameter 2.5 cm; thickness 1 mm) were mounted on a rotable support plate 5–6 cm below the targets and oriented perpendicular[12] to the target surfaces. During the deposition, the substrates revolved by 144 rpm, which is sufficient for uniform mixing of ZnO and Al. The deposition rate was 0.11–0.13 nm s^{-1}. Film thicknesses lay in the 78–330-nm interval, as found by surface profilometry. Quantitative elemental analysis was accomplished by Rutherford backscattering spectrometry on ZnO:Al films deposited onto Be foil. The Al content was found to be $\lesssim 2$ at. %.

Optical properties were measured in the 2–5-eV energy range. We used a Beckman ACTA MVII double-beam spectrophotometer, interfaced to a computer, to record normal transmittance T and near-normal reflectance R. An Al reference mirror, taken to have bulklike optical properties, was used in the determination of R. Figure 1 shows data for a 330-nm thick ZnO:Al film containing ~ 2.14 at. % Al. A large drop of T around 3.5 eV indicates the band gap. Oscillations in T and R are caused by optical interference.

Spectrophotometric data of the kind shown in Fig. 1 were used to determine the complex dielectric function. The evaluation was based on Fresnel's equations[13] and known[14] optical properties of CaF_2. The screened plasma energy $\hbar\omega_p$ was then obtained from the condition that the real part of the dielectric function equals zero. The electron density n_e is related to ω_p by

$$n_e = \omega_p^2 \epsilon(\infty) m_e / (4\pi e^2) , \quad (1)$$

where $\epsilon(\infty)$ is the high-frequency dielectric constant, m_e is the effective mass for electrons in the conduction band, and e is the electron charge. Tabulated[9] data for ZnO yield $m_e = 0.28m$, where m is the free-electron mass and $\epsilon(\infty) = 3.85$. Table I gives n_e's for four different films with different amounts of Al. Depending on the Al content, the electron density lies in the $(1-5)\times 10^{20}$ cm^{-3} interval. The Al atoms are expected[15] to enter substitutionally on Zn sites in the ZnO lattice so that they act as singly ionized donors. Doping of pure ZnO is likely to be associated with oxygen deficiency.

The spectral absorption coefficient was calculated from the dielectric function of the ZnO:Al films. Figure 2 shows results for four samples with different degrees of doping. The optical band-gap E_g was associated[1] with the energy corresponding to the maximum $d\alpha/d(\hbar\omega)$. As seen from Table I, E_g goes from ~ 3.4 eV at low doping up to as much as ~ 3.9 eV at the highest doping. Stoichiometric ZnO crystals have $E_g = 3.4$ eV (Ref. 9). The band-gap widening is accompanied by a smearing of

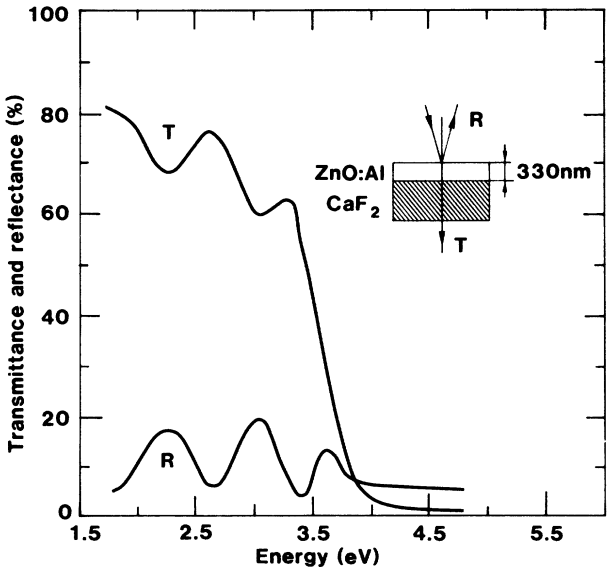

FIG. 1. Spectral transmittance at normal incidence and reflectance at 10° angle of incidence for a ZnO:Al film on CaF_2. The measurement configuration is indicated in the inset.

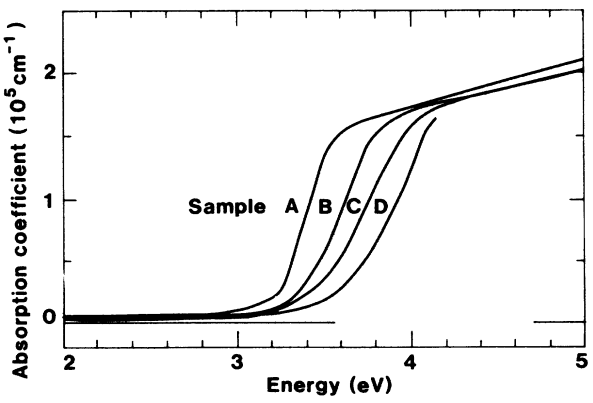

FIG. 2. Spectral absorption coefficient for films of ZnO (sample *A*) and ZnO:Al (samples *B*–*D*). Sample data are given in Table I.

the transition between low and high absorption. Earlier data on band-gap widening have been reported for films of nonstoichiometric ZnO (Refs. 16 and 17), and ZnO doped by Al (Ref. 12), Si (Ref. 18), and In (Ref. 19). The scatter in the literature data is too large to make a comparison with our results meaningful.

III. THEORY OF BAND-GAP SHIFTS

The optical gap is defined as the minimum energy needed to excite an electron from the valence band to the conduction band. In the pure, undoped crystal the optical gap equals the energy separation E_{g0} between the band edges, as illustrated for the case of isotopic and parabolic bands in Fig. 3(a). In a heavily doped semiconductor, the donor electrons occupy states at the bottom of the conduction band. Since the Pauli principle prevents states from being doubly occupied and optical transitions are vertical, the optical gap is given by the energy difference between states with Fermi momentum in the conduction and valence bands. This is shown in Fig. 3(b). The blocking of the low-energy transitions is known as the Burstein-Moss (BM) effect and enhances the optical gap by the energy

$$\Delta E_g^{\mathrm{BM}}=\frac{\hbar^2 k_F^2}{2}\left[\frac{1}{m_e}+\frac{1}{m_h}\right], \tag{2}$$

where k_F is the Fermi wave vector, and m_h is the effective mass for holes in the valence band. The band-gap widening is counteracted by a narrowing caused by the correlated motion of the charge carriers and by their scattering against ionized impurities. The ensuing effect on the optical gap is given, schematically, in Fig. 3(c). The rest of this section is devoted mainly to quantitative assessments of band-gap narrowing.

We first consider a *nonpolar* semiconductor. Its electrons avoid each other for two different reasons: Electrons of equal spin avoid each other for statistical reasons, and all electrons—irrespective of relative spin—avoid each other because of Coulomb repulsion. Thus, effectively each electron is surrounded by an exchange and correlation hole which lowers the energy of the electron, i.e., the conduction band is shifted downwards. Furthermore, the electron density will relax around the impurities, which causes a lowering of the electron energies and an additional downward shift of the conduction band. This latter shift is nonrigid because the interaction will in general give rise to a distorted band structure and band tailing.

The valence band is also shifted, as can be understood from the following argument: Experiments measuring band-gap shifts involve a hole in the valence band and an electron in the conduction band. In absorption experiments such electron-hole pairs are created, and in luminescence experiments electron-hole pairs are annihilated. The hole is attracted by the donor electrons and tends to be surrounded by an enhanced electron density. This lowers the energy of the hole. The hole is repelled by the positively charged donor ions and has a tendency to avoid them, which causes a further downward shift of its energy. Thus even less energy is needed to create an electron-hole pair or is released when a pair is annihilated. In other words, the valence band is shifted upwards in energy.

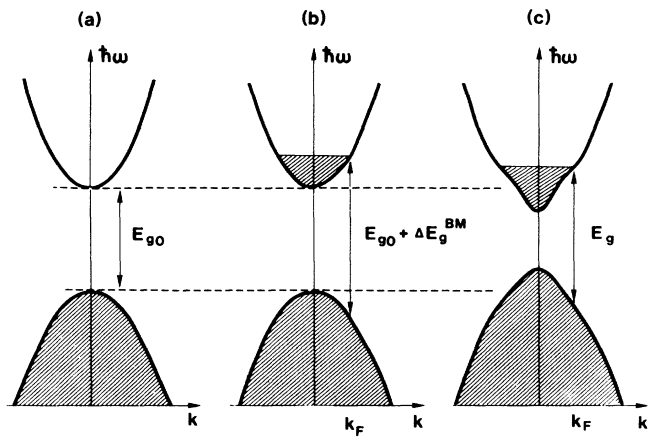

FIG. 3. Schematic band structure with parabolic conduction and valence bands separated by E_{g0} [part (a)], after heavy doping assumed to have the sole effect of blocking the lowest states in the conduction band so that the optical gap is widened by a Burstein-Moss shift ΔE_g^{BM} [part (b)], and representation of a perturbed band structure and ensuing optical band gap E_g in the case of many-body interactions [part (c)]. Shaded areas denote occupied states. The Fermi wave vector k_F is indicated.

In a *polar* semiconductor, or ionic insulator, there is a displacement of charge from one of the atomic species to the other, and hence the host atoms are charged. A moving charged particle then causes a displacement polarization, which follows the particle in the crystal. An electron attracts the positively charged atoms and repels the negatively charged ones. Effectively, an electron is surrounded by a cloud of positive charge, and the valence-band hole is surrounded by a cloud of negative charge. The particle and its charge cloud can be viewed as a new particle, a polaron.

The displacement polarization modifies the self-energy shifts caused by the many-body interactions. The details of the derivation of these shifts can be found in Ref. 6. Here we just give the final result, which for a state p is

$$\Sigma_p^{\mathrm{int},j}=-\frac{1}{\Omega}\sum_{\mathbf{q}}{}'\,v(q)\int_{-\infty}^{\infty}d\omega\frac{1}{2\pi i}\left\{\frac{1}{\epsilon_L(\omega)}\left[G_0^j(\mathbf{p}+\mathbf{q},\,e_p^j/\hbar+\omega)/\epsilon(\mathbf{q};\omega)+\frac{1}{2}\left[\frac{1}{\omega+\omega^j(\mathbf{p},\mathbf{q})-i\eta}-\frac{1}{\omega-\omega^j(\mathbf{p},\mathbf{q})+i\eta}\right]\right]\right.$$
$$\left.-\left[\frac{1}{\epsilon_L(\omega)}-\frac{1}{\epsilon(\infty)}\right]\frac{1}{2}\left[\frac{1}{\omega+\omega^j(\mathbf{p},\mathbf{q})-i\eta}-\frac{1}{\omega-\omega^j(\mathbf{p},\mathbf{q})+i\eta}\right]\right\}, \tag{3}$$

where j stands for e or h, representing a conduction-band electron or a valence-band hole, respectively, and Ω is the total volume of the system, $v(q)$ is the Fourier transform of the Coulomb potential, $\epsilon_L(\omega)$ is the lattice dielectric function, G_0 is a (noninteracting) Green's function, e_p is the kinetic energy for a particle in state $\mathbf{p}$, $\epsilon(\mathbf{q};\omega)$ is the dielectric function for a degenerate electron gas (given by the random-phase approximation[7]), and $\hbar\omega(\mathbf{p},\mathbf{q})$ is the change of kinetic energy for a particle in going from state $\mathbf{p}$ to state $\mathbf{p}+\mathbf{q}$. The first term in the curly brackets in Eq. (3) can be viewed as a contribution from the interaction of the polaron in state $\mathbf{p}$ with the rest of the polarons. Hence, it is the exchange and correlation contribution for the polaron. The last term in the curly brackets represents the energy contained in the polaron itself. It stems from the reduction in energy caused by the host atoms adjusting their positions to the potential from the moving charged particle. For the state $p=0$, this represents the polaron ground state, which can be expressed as

$$E^j_{\rm pol}=e^2\left[\frac{m_j\omega_L}{2\hbar}\right]^{1/2}\left[\frac{1}{\epsilon(0)}-\frac{1}{\epsilon(\infty)}\right]=-\alpha_j\hbar\omega_L\ . \quad (4)$$

Here α_j is the coupling constant for a polaron of type j, $\hbar\omega_L$ is a characteristic phonon energy, and $\epsilon(0)$ is the low-frequency dielectric constant. Clearly, the polaron energy depends on the effective mass and is different for the conduction and valence band. The two polaron ground-state energies are contained in the measured band-gap of the undoped crystal, and hence must be subtracted in an expression for the band-gap shift.

The self-energy shifts caused by interactions with the dopant atoms can be written

$$\Sigma^{{\rm ion},j}_p=\frac{N}{\hbar\Omega}\sum_{\mathbf{q}}{}'\left[\frac{v(q)}{\epsilon(0)\epsilon(\mathbf{q},0)}\right]^2 G^j_0(\mathbf{p}+\mathbf{q},\, e^j_p/\hbar)\ , \quad (5)$$

where N is the ion density. In the case of single ionization, we have $N=n_e$. Equation (5) is the same expression[20] as for a nonpolar semiconductor, except that $\epsilon(0)$ is used to describe the background screening.

It is now possible to give an expression for the optical gap, viz.,

$$E_g=E_{g0}-E^e_{\rm pol}-E^h_{\rm pol}+\Delta E^{\rm BM}_g + {\rm Re}(\Sigma^{{\rm int},e}_{k_F}+\Sigma^{{\rm ion},e}_{k_F}+\Sigma^{{\rm int},h}_{k_F}+\Sigma^{{\rm ion},h}_{k_F})\ . \quad (6)$$

The first three terms represent the band-gap of the undoped crystal in the absence of displacement polarization. The four self-energy terms are all negative and lead to a band-gap narrowing. In the present case interaction effects dominate by far over effects of impurity scattering.

IV. COMPARISON OF THEORY AND EXPERIMENTS

The experimental results of Sec. II will now be compared with the theory outlined in Sec. III. Solid circles in Fig. 4 show experimental data on the optical gap as a function of electron density. Several of the points represent data reported in Table I. Error bars signify the uncertainty in the determination of the optical gap. Curves in Fig. 4 show computed results. In order to make the theory applicable to doped ZnO, we set $m_e=0.28m$, $m_h=0.59m$, $\epsilon(\infty)=3.85$, $\epsilon(0)=8.0$, and $\hbar\omega_L=72$ meV. All of these quantities were taken from Ref. 9. Further we used $E_{g0}=3.38$ eV, which fixes the energy scale for the optical gap. This value of E_{g0} is in excellent accord with the band-gap reported[9] for stoichiometric ZnO.

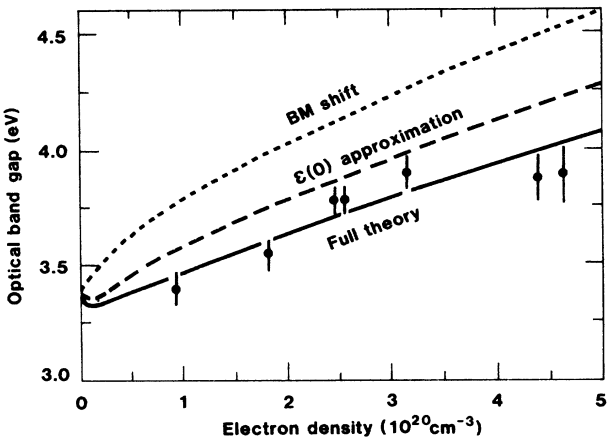

FIG. 4. Optical band-gap vs electron density for ZnO:Al films as obtained from experimental data (solid circles) and as computed (curves). Solid curve refers to the theory for polar semiconductors outlined above, dashed curve is valid for the $\epsilon(0)$ approximation used in Ref. 1, and the dotted curve applies to the simple Burstein-Moss shift. The computations are valid only well above the Mott critical density, i.e., at $n_e \gg 10^{19}$ cm^{-3}, although theoretical values are plotted also for lower densities. (For small electron concentrations the two models including self-energy shifts predict that the optical band-gap initially decreases.)

The experimental data are seen to agree very well with the solid curve obtained by using the full theory of band-gap in a polar semiconductor. In order to appreciate this agreement, we also present theoretical results obtained from two simplified theories. The first of these, called the $\epsilon(0)$ approximation, is the one used in our earlier work.[1] It is here represented by the dashed curve. This approximation regards the semiconductors as being nonpolar but with a background screening constant equal to $\epsilon(0)$. It is found that this simplified theory can be reconciled with the experiments only by taking $E_{g0}\approx 3.15$ eV, which is far too low to be credible. Considering, finally, only the Burstein-Moss shift[3] yields the dotted curve, which is in severe disagreement with the experimental results. In conclusion, we find that the theory[6] for band-gap shifts in polar semiconductors gives a quantitative description of the experimentally found widening of the optical gap in Al-doped ZnO films.

ACKNOWLEDGMENTS

This work was financially supported by grants from the Swedish Natural Science Research Council and the National Swedish Board for Technical Development. It was further supported by the Division of Materials Sciences, U.S. Department of Energy, under Contract No. DE-AC05 84 0R 21400 with Martin Marietta Energy Systems, Inc., and the University of Tennessee.

*Present address: Theoretical Physics Group, Department of Physics and Measurement Technology, Linköping University, S-581 83 Linköping, Sweden.

†Permanent address: Department of Applied Physics, Beijing Polytechnic University, Beijing, People's Republic of China.

‡Present address: Process Development, Ericsson Components, S-163 81 Stockholm, Sweden.

[1]I. Hamberg, C. G. Granqvist, K.-F. Berggren, B. E. Sernelius, and L. Engström, Phys. Rev. B **30**, 3240 (1984); I. Hamberg and C. G. Granqvist, J. Appl. Phys. **60**, R123 (1986).

[2]N. F. Mott, *Metal-Insulator Transitions* (Taylor and Francis, London, 1974).

[3]E. Burstein, Phys. Rev. **93**, 632 (1954); T. S. Moss, Proc. Phys. Soc. London, Ser. B **67**, 775 (1954).

[4]R. A. Abram, G. J. Rees, and B. L. H. Wilson, Adv. Phys. **27**, 799 (1978).

[5]K.-F. Berggren and B. E. Sernelius, Phys. Rev. B **24**, 1971 (1981).

[6]B. E. Sernelius, Phys. Rev. B **36**, 4878 (1987), and references therein.

[7]G. D. Mahan, *Many Particle Physics* (Plenum, New York, 1981).

[8]W. Hirschwald *et al.*, in *Current Topics in Materials Science,* edited by E. Kaldis (North-Holland, Amsterdam, 1981), Vol. 7, pp. 143–482.

[9]*Numerical Data and Functional Relationships in Science and Technology,* Vol. 17b of *Landolt-Börnstein New Series,* edited by O. Madelung, M. Schulz, and H. Weiss (Springer-Verlag, Berlin, 1982), p. 35; Vol. III, Teil 22a of *Landolt-Börnstein New Series,* edited by O. Madelung and M. Schulz (Springer-Verlag, Berlin, 1987), p. 160.

[10]Z.-C. Jin, I. Hamberg, and C. G. Granqvist, Appl. Phys. Lett. **51**, 149 (1987); Z.-C. Jin and C. G. Granqvist, Appl. Opt. **26**, 3191 (1987), Proc. Soc. Photo-Opt. Instrum. Engr. (to be published).

[11]T. S. Eriksson and C. G. Granqvist, J. Appl. Phys. **60**, 2081 (1986).

[12]T. Minami, H. Nanto, and S. Takata, Jpn. J. Appl. Phys. **23**, L280 (1984); **24**, L605 (1985); Thin Solid Films **124**, 43 (1985); T. Minami, H. Sato, H. Nanto, and S. Takata, Jpn. J. Appl. Phys. **24**, L781 (1985).

[13]M. Born and E. Wolf, *Principles of Optics,* 6th ed. (Pergamon, New York, 1983).

[14]Results obtained from the Harshaw Chemical Company.

[15]G. Neumann, in Ref. 8, pp. 153-168.

[16]A. P. Roth, J. B. Webb, and D. F. Williams, Phys. Rev. B **25**, 7836 (1982).

[17]O. Caporaletti, Solar Energy Mater. **7**, 65 (1982).

[18]T. Minami, H. Sato, H. Nanto, and S. Takata, Jpn. J. Appl. Phys. **25**, L776 (1986).

[19]S. Major, A. Banerjee, and K. L. Chopra, J. Mater. Res. **1**, 300 (1986).

[20]B. E. Sernelius, Phys. Rev. B **34**, 5610 (1986).